Hybrid Filtered Multitone Architecture for WLAN Applications

Salvatore D'Alessandro, Nicola Moret, Andrea M. Tonello
DIEGM Universitá di Udine, Udine, Italy
Email: {salvatore.dalessandro, nicola.moret, tonello}@uniud.it;

***Abstract*—In this paper we propose a novel hybrid multi-carrier architecture for wireless LAN (WLAN) applications. We refer to this architecture as hybrid filtered multitone (H-FMT). Depending on the experienced channel condition, H-FMT switches between short orthogonal FMT (SO-FMT) modulation, and adaptive orthogonal frequency division multiplexing (A-OFDM). Extensive numerical results show that H-FMT could significantly improve the capacity and the robustness of the WLAN standard that deploys conventional OFDM. Furthermore, its efficient implementation has a complexity that is comparable to that of OFDM.**

I. Introduction

In multi carrier (MC) transmission schemes [1], a broadband signal is converted into M narrow band signals such that each of them experiences a near flat frequency response, permitting to considerably ease the equalization task.

In this paper we consider two forms of MC modulation that are respectively short orthogonal FMT (SO-FMT) and adaptive OFDM (A-OFDM).

The FMT system is a discrete-time implementation of MC modulation that uses uniformly spaced sub-carriers and identical sub-channel pulses. OFDM can be viewed as an FMT scheme that deploys rectangular time domain filters. FMT has been originally proposed for application in broadband wireline channels [2], and subsequently it has been investigated for application in wireless channels [3],[4]. There are several design approaches for the FMT systems: the first one uses a frequency confined prototype pulse to make the sub-channels quasi-orthogonal to each other, and to use sub-channel equalizers to cope with the inter-symbol interference (ISI) introduced by the channel. This approach requires long prototype pulses that render negligible the inter channel interference (ICI), but increase considerably the computational complexity [3]-[6]. A different design technique is to use short filters with minimal length equal to the duration of one transmitted symbol, which are designed to be perfectly orthogonal in ideal conditions, and to be maximally confined in frequency [7]. This approach allows keeping low both the complexity and the inter-channel interference (ICI). We name this scheme as SO-FMT.

As mentioned above, the OFDM system uses a rectangular impulse response prototype pulse. It is well known that in presence of frequency selective channel, the cyclic prefix (CP) is needed to mitigate the interference components. If the CP is longer than the channel impulse response, the system maintains its orthogonality properties, thus, no interference is present at the decision stage. Nevertheless, this benefit is paid in term of a loss in achievable rate and signal over noise ratio (SNR) of a factor $M/(M+\beta)$, where M denotes the number of sub-channels and β the CP length in samples. Clearly, when the CP is shorter than the channel duration ISI and ICI terms arise [8].

In our previous work [9], we have found that over typical WLAN channels, the CP has not to be necessarily as long as the channel duration to maximize the achievable rate. Furthermore, for each channel class of the IEEE 802.11n WLAN channel model [10], we have found a nearly optimal value of CP designed according to the statistic of the capacity-optimal CP duration. We have shown that capacity improvements for the WLAN standard are attainable adapting the CP to the experienced channel class, this is true for both the single and the multi user cases. We refer to the OFDM that adapts the CP to the channel condition as A-OFDM.

Comparing the performance of SO-FMT and A-OFDM, we have found that depending on the channel condition it is convenient to use one scheme rather than the other. Therefore, in this paper we propose to exploit the similarities of both schemes using the hybrid architecture H-FMT. This new scheme wisely switches between SO-FMT and A-OFDM depending on the experienced channel. Thanks to the similarities of the efficient implementation of both SO-FMT and A-OFDM [11], the efficient implementation of H-FMT introduces a marginal increase of the computational complexity w.r.t. the conventional OFDM. The performance improvements that are attainable with H-FMT are studied for the WLAN application scenario. It is worth noting that the use of hybrid schemes seems to be a new direction for next telecommunication systems. In fact, new home networking standards as IEEE P1901 and ITU G.hn [12] propose the use of different modulation techniques, e.g., IEEE P1901 allows the use of both OFDM and wavelet OFDM. Furthermore, also the research interest for the hybrid architectures is increasing. As an example, in [13] a hybrid architecture based on hermitian symmetry - offset quadrature amplitude modulation (HS-OQAM) and discrete multitone (DMT) modulation is proposed for communication over power line channels.

The paper is organized as follows. In Sec. II we present the general system model. Then, in Sec. III and IV we

The work of this paper has been partially supported by the European Community's Seventh Framework Programme FP7/2007-2013 under grant agreement n. 213311, project OMEGA – Home Gigabit Networks.

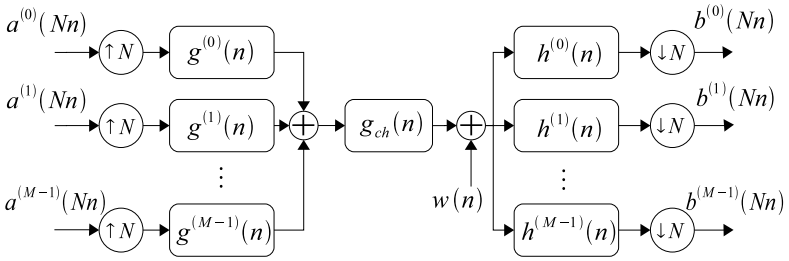

Fig. 1. General filter bank architecture.

briefly recall the SO-FMT and the A-OFDM systems and their principles. In Sec. V we present the novel H-FMT architecture. In Sec. VI we report extensive numerical results showing that over typical WLAN channels [10] the use of H-FMT increases the system capacity and further renders the system more reliable than the conventional OFDM adopted in the WLAN standard [14]. Finally, in Sec. VII the conclusions follow.

II. System Model

We consider a general MC scheme as depicted in Fig. 1 where the high rate discrete-time transmitted signal at the output of the synthesis filter bank (FB), $x(n)$, is obtained by the modulation of M data streams at low rate $a^{(k)}(Nn)$, with $k \in \{0, \cdots, M-1\}$, that belong to a constellation signal set (e.g., quadrature amplitude modulation). The transmitted signal can be written as

$$x(n) = \sum_{k=0}^{M-1} \sum_{l \in \mathbb{Z}} a^{(k)}(Nl) g^{(k)}(n - Nl), \tag{1}$$

where M is the number of sub-channels, $N = M + \beta$ is the sampling-interpolation factor, with β equal to the overhead (OH) duration in samples. According to (1), the signals $a^{(k)}(Nn)$ are upsampled by a factor N and are filtered by the modulated pulses $g^{(k)}(n) = g(n) W_M^{-kn}$, with $g(n)$ being the prototype filter of the synthesis bank and $W_M^{kn} = e^{-j\frac{2\pi}{M}kn}$. Then, the sub-channel signals are summed and transmitted over the channel.

We use the IEEE 802.11 TGn [10] channel model. This model generates channels belonging to five classes labeled with B,C,D,E,F. Each class is representative of a certain environment, e.g., small office, large open space/office with line of sight (LOS) and non LOS (NLOS) propagation, and so on. Both small scale multipath fading and large scale path loss fading as a function of distance are taken into account. Although the model allows considering MIMO channels, we restrict ourselves to the case of single-transmit/single-receive antenna. For a detailed description of the model, see [10] and [9].

After propagation through the channel and with the addition of white Gaussian noise, the received signal $y(n)$ is processed by the analysis FB whose outputs are

$$b^{(k)}(Nn) = \sum_{m \in \mathbb{Z}} y(m) h^{(k)}(Nn - m). \tag{2}$$

According to (2), the signal $y(n)$ is filtered by the modulated pulses $h^{(k)}(n) = h(n) W_M^{-kn}$ with $h(n)$ being the prototype pulse of the analysis bank, and are downsampled by a factor N.

In order to evaluate the system performances, we assume parallel Gaussian channels and independent and Gaussian distributed input signals, which render ISI and ICI also Gaussian (cf. e.g. [8]). Therefore, the achievable rate in bit/s for a given channel realization, and supposing single tap zero forcing equalization, is given by

$$C(\beta) = \frac{1}{(M+\beta)T} \sum_{k=0}^{M-1} \log_2 \left(1 + SINR^{(k)}(\beta)\right), \tag{3}$$

where $SINR^{(k)}(\beta)$ denotes the signal over interference plus noise ratio experienced in sub-channel k when we transmit using an overhead of β samples. It is defined as

$$\begin{aligned} SINR^{(k)}(\beta) &= \frac{P_{\mathrm{U}}^{(k)}(\beta)}{P_{\eta}^{(k)} + P_{\mathrm{I}}^{(k)}(\beta)} \\ &= \left(\frac{1}{SNR^{(k)}(\beta)} + \frac{1}{SIR^{(k)}(\beta)} \right)^{-1}, \end{aligned} \tag{4}$$

where $P_{\mathrm{U}}^{(k)}(\beta)$, $P_{\mathrm{I}}^{(k)}(\beta)$ and $P_{\eta}^{(k)}$ respectively denote the useful, the interference, and the noise power terms on sub-channel k. Details on their computation can be found in [15]. In (4), the terms SNR and signal over interference ratio (SIR) are defined as $SNR^{(k)}(\beta) = P_{\mathrm{U}}^{(k)}(\beta)/P_{\eta}^{(k)}$ and $SIR^{(k)}(\beta) = P_{\mathrm{U}}^{(k)}(\beta)/P_{\mathrm{I}}^{(k)}(\beta)$. In (3), T denotes the sampling factor.

In the next two sections we derive FMT and OFDM from the general MC scheme.

III. Short Orthogonal FMT (SO-FMT)

The SO-FMT scheme can be obtained from the general system model simply substituting the prototype pulse $g(n) = h^*(-n)$ with an FMT orthogonal pulse having minimal length. These pulses satisfy the orthogonality conditions given by the following system of equations

$$\begin{aligned} \left[g^{(k)} * h^{(i)} \right](Nn) &= \delta_n \, \delta_{i-k}, \\ &\forall (k,i) \in \{0, \cdots, M-1\}, \ \forall n \in \mathbb{Z}, \end{aligned} \tag{5}$$

where we denote with δ_n the Kronecker delta. The solution of this system is not unique, and thus we parameterize the filter coefficients with a minimal set of parameters θ. In order to

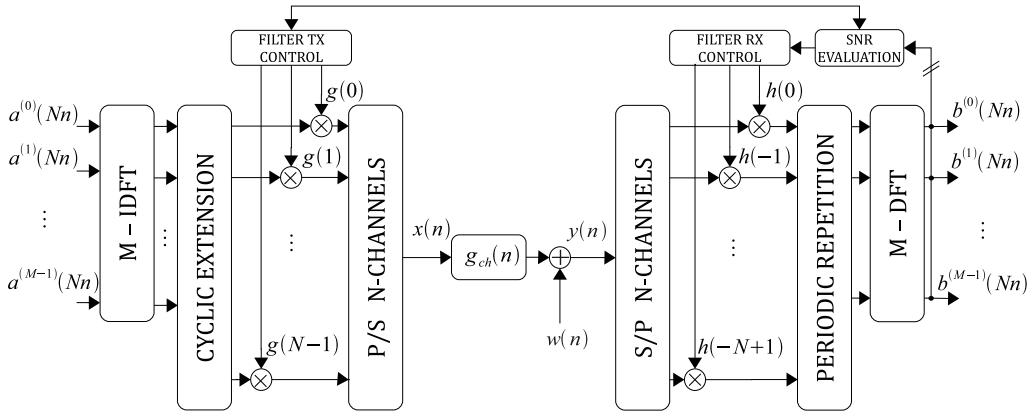

Fig. 2. Hybrid FMT scheme.

have maximally frequency confined pulses, we choose those parameters θ that satisfy the minimum square error from a target pulse $H(f)$:

$$\arg\min_{\theta} \int_{-.5}^{.5} |G(f,\theta) - H(f)|^2 df, \tag{6}$$

where $G(f,\theta)$ is the frequency response of the prototype pulse $g(n)$ as function of the parameters θ. It is worth noting that the choice of the filter determines the achievable rate (3) inasmuch it is proportional to the overhead $\beta = N - M$, therefore β can be adapted to the channel condition to maximize the achievable rate. Nevertheless, in order to keep low the system implementation complexity, the family of filters adopted in this paper has minimal length equal to one symbol duration, i.e., $L_g = N$. The interpolation factor is equal to $N = \frac{2^p+1}{2^p}M$, $p = 3$. More details regarding the filter design for SO-FMT are reported in [7].

IV. Adaptive OFDM (A-OFDM)

The OFDM scheme can be obtained setting the synthesis and the analysis pulses respectively equal to

$$g(n) = \frac{1}{\sqrt{N}}\, rect\,(n/N)\,, \tag{7}$$
$$h(n) = \frac{1}{\sqrt{M}}\, rect\,(-n/M)\,,$$

where $rect\,(n/A) = 1$ for $n = \{0, 1, \ldots, A-1\}$ and zero otherwise. The factor β denotes the length of the CP. As previously said, when the length of the CP is greater than the channel duration, the received signal is neither affected by ISI nor by ICI [8].

As we have shown in our previous work [9], the CP has not to be necessarily as long as the channel duration to maximize the achievable rate (3). Furthermore, since the achievable rate is not a convex function of the CP duration, the optimal approach to find the CP that maximizes (3) requires an exhaustive search over the set of values $0, \ldots, L_{ch} - 1$, where L_{ch} denotes the channel duration in samples, namely

$$\beta_{opt} = \underset{\beta \in \{0,\ldots,L_{ch}-1\}}{\operatorname{argmax}} \{C(\beta)\}\,. \tag{8}$$

A significant simplification that assures the feasibility of the CP adaptation to the channel realization, is to pre-compute a limited amount of CP values, and then adapt the CP over this small set. In [9] we have found such a limited set studying the statistic of the optimal CP duration. We have denoted this set as $\mathbb{P}_{OFDM} = \left\{\beta_B^{(99\%)}, \beta_C^{(99\%)}, \beta_D^{(99\%)}, \beta_E^{(99\%)}, \beta_F^{(99\%)}\right\}$. That is, depending on the experienced channel class, the adaptive OFDM picks the corresponding CP value from the set $\mathbb{P}_{OFDM}$. In [9] we have shown that the CP adaptation over the set $\mathbb{P}_{OFDM}$ gives negligible achievable rate loss w.r.t. the optimal approach (8), and further it significantly increases the system performances w.r.t. the use of OFDM with a fixed and conservatively long CP.

V. Hybrid FMT (H-FMT)

In this section we describe a novel MC architecture able to exploit the strong points of both SO-FMT and A-OFDM.

To motivate the use of such scheme we make the following observations. We have numerically found that over typical WLAN channels, A-OFDM and SO-FMT respectively experience an interference level which is in average 80 dB and 40 dB under the level of the useful signal (see Section VI). Besides, we note that in A-OFDM the analysis and the synthesis pulses are not matched. This causes a loss in SNR of a factor $M/(M+\beta)$ w.r.t. SO-FMT. Having said that, we observe that when the channel attenuation is high, and both systems are noise limited, the SINR (4) can be approximated with the SNR. Consequently, in such a case (supposing the OH of FMT shorter or equal to the CP of OFDM) the use of FMT gives an higher value of achievable rate than the one obtained with A-OFDM (see (3)). In other words, when the SNR is low it is better to use FMT than OFDM. On the contrary, when the channel attenuation is low, namely when the SNR is high, and both systems are interference limited, the SINR (4) can be approximated with the SIR. In such a case, the interference experienced by SO-FMT is higher than the one of A-OFDM and thus the use of SO-FMT gives lower achievable rate than A-OFDM. It is therefore justified the use of a hybrid architecture able to dynamically switch, according

to the channel condition, between SO-FMT and A-OFDM. We call such an architecture H-FMT.

We propose to implement the H-FMT using the efficient implementation of a DFT modulated filter bank proposed in [11]. Fig. 2 shows the H-FMT architecture. As we can see, at the transmitter the M data signals are processed by an M points IDFT. The N output samples from the cyclically extension, are multiplied by the coefficients $g(n)$, with $n = 0, \ldots, N-1$. $g(n)$ correspond to the prototype synthesis pulse coefficients of SO-FMT or A-OFDM. Finally, the outputs are parallel-to-serial converted. The receiver comprises the following operations. The signal is serial-to-parallel converted with a converter of size N. Depending on the modulation scheme used at the transmitter, namely SO-FMT or A-OFDM, the output signals are multiplied by the corresponding prototype analysis pulse coefficients $h(-n)$ with $n = 0, \ldots, N-1$. Then, the periodic repetition with period M of the block of coefficients of size N is applied. Finally, the M-point DFT is performed. Note that the A-OFDM analysis pulse has length M which is shorter than the pulse used for the synthesis stage with length N, but it can be considered with length N simply padding β zeros.

The choice about the usage of A-OFDM or SO-FMT (see Sec. VI) is made by the block SNR Evaluation. That is, depending on the experienced SNR, this block selects the appropriate modulation scheme and accordingly the TX and RX controllers set the corresponding coefficients $g(n)$ and $h(n)$ at the transmitter and at the receiver side. Note that the SNR evaluation can be done using OFDM with a CP longer than the channel duration. In this case the received signal results free of interference and the SINR (4) corresponds to the SNR. Furthermore, to adapt the system to the channel condition, the SNR evaluation is done periodically.

Taking into account that in SO-FMT only β coefficients of the prototype pulse differ from a constant, the complexity of this scheme is $(\alpha M \log M + \beta)/N$, and $(\alpha M \log M + 2\beta)/N$ operation per sample for the synthesis and the analysis stages respectively where the α factor takes into account the FFT implementation. Hence, the complexity of H-FMT is almost the same of the efficient implementation of OFDM which is $(\alpha M \log M)/N$ for both synthesis and analysis stages.

VI. Numerical Results

To obtain numerical results, we have chosen the following system parameters that are essentially those of the IEEE 802.11 standard [14]. The MC system uses $M = 64$ sub-channels with a transmission bandwidth of 20 MHz. The signal is transmitted with a constant power spectral density (PSD) of -53 dBm/Hz. At the receiver side, we add white Gaussian noise with PSD equal to -168 dBm/Hz. Thus, the SNR, without path loss and fading, on each sub-channel is 115 dB. To show the performance of H-FMT, we use an OFDM baseline system which deploys a fixed CP of 0.8 μs ($\beta = 16$ samples), that is the value of CP employed in the IEEE 802.11 standard [14].

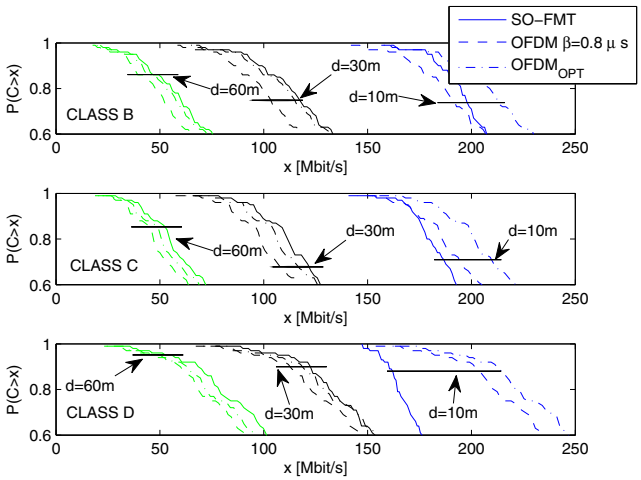

Fig. 3. Achievable rate CCDF obtained using SO-FMT, A-OFDM, and OFDM with a fixed CP of 0.8 μs. The employed channel classes are the B,C, and D. The distance between transmitter and receiver is set to 10 m, 30 m, and 60 m.

The H-FMT deploys SO-FMT with fixed OH of 0.4 μs ($\beta = 8$ samples, $N = 9/8M$), and A-OFDM with values of CP equal to $\mathbb{P}_{OFDM} = \{\beta_B^{(99\%)} = 0.4\mu s, \beta_C^{(99\%)} = 0.5\mu s, \beta_D^{(99\%)} = 0.6\mu s, \beta_E^{(99\%)} = 0.9\mu s, \beta_F^{(99\%)} = 1.1\mu s\}$ [9]. Both schemes use single tap zero forcing sub-channel equalization.

Fig. 3 shows the complementary cumulative distribution function (CCDF) of the achievable rate obtained using SO-FMT, A-OFDM, and the baseline system. For the sake of readability, we only show results for channel classes B, C, and D and for distances between transmitter and receiver equal to 10 m, 30 m, and 60 m. More results for the baseline OFDM and for A-OFDM can be found in [9]. From Fig. 3 we can observe how for high values of distance $d = \{30, 60\}m$, and thus in the low SNR region, the SO-FMT shows better performance than both A-OFDM and baseline OFDM. On the contrary, for a short distance of 10 m, A-OFDM is able to achieve higher rate than FMT. Although not shown, the results obtained with a distance of 3 m behave as the ones obtained with a distance of 10 m. From Fig. 3 we notice that with probability 0.9, the average gain obtained using SO-FMT and A-OFDM w.r.t. the baseline system is respectively of 17.3% and 8.3% at a distance of 60 m, of 13.4% and 8.7% at a distance of 30 m, and of -5% and 5% at a distance of 10 m.

In Fig. 4 we report the average SNR for each channel class and for distances between transmitter and receiver of 3 m, 10 m, 30 m, and 60 m. Each point has been computed as the ratio between the power of the transmitted signal attenuated by the average channel path loss, and the power of the noise. It is worth noting that the SNR experienced by SO-FMT corresponds to the showed one. Whereas, to obtain the SNR experienced by A-OFDM, we must lower the showed SNR of a factor $10log_{10}(M/(M+\beta))$. For instance, for the highest used value of OH $\beta_F^{(99\%)} = 1.1\mu s$ (22 samples) we have to lower the SNR of Fig. 4 by 1.28 dB. Fig. 4 also shows the average SIR (averaged across all the channel classes and

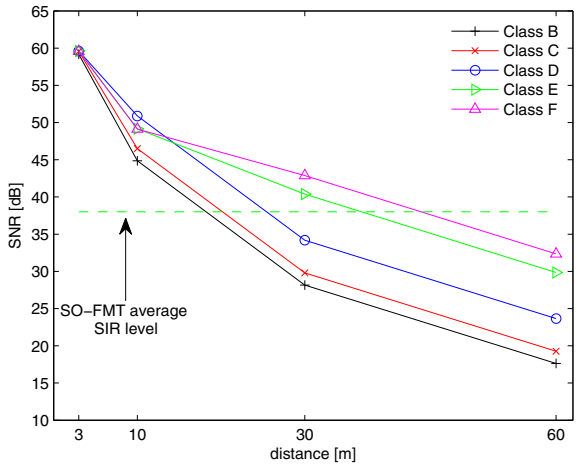

Fig. 4. SNR as function of the distance, and mean value of SIR for the SO-FMT.

across all the distances) of the SO-FMT. Regarding A-OFDM, it always experiences a SIR that is several dBs higher than the one of SO-FMT.

Now the question is: *how does the system select the modulation to be used*? Looking at Fig. 4 and thus focusing of SO-FMT, we observe that when the SNR is higher than the SIR, the SINR (4) can be approximated by the SIR. Recalling that the SIR of A-OFDM is higher than that of SO-FMT, we deduce that in such a case is better to use A-OFDM than SO-FMT. Viceversa, when the SNR is lower than the SIR, the SINR (4) can be approximated by the SNR. Recalling that the SNR of A-OFDM is lower than that of SO-FMT, we deduce that in such a case is better to use SO-FMT than A-OFDM.

Summarizing, when the SNR is below the SIR line of Fig. 4 it is convenient to use SO-FMT. Otherwise, we use A-OFDM.

Fig. 5 shows the achievable rate CCDF for the baseline system and for H-FMT. The simulated channel classes are

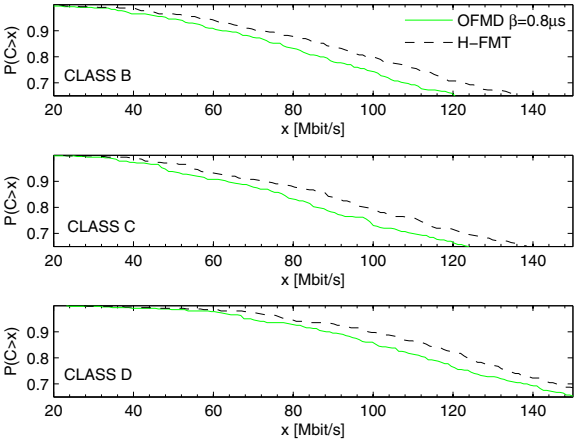

Fig. 5. Achievable rate CCDF using H-FMT and OFDM with fixed CP equal to 0.8 μs for channel class B, C, and D.

the B, C, and D. For each class, the curves are computed considering random distances from the set $\{3, 10, 30, 60\}m$. We notice that with probability 0.9, H-FMT provides gains in achievable rate of $\{16\%, 15\%, 12\%\}$ w.r.t. OFDM for channel classes B, C, and D respectively. More precisely, with probability 0.9, for channel classes B, C, and D, OFDM exceeds $\{60, 64, 85\}Mbit/s$, while H-FMT exceeds $\{72, 74, 98\}Mbit/s$.

Finally, looking at Fig. 3, it should be noted that also if not explicitely highlighted before, the achievable rate CCDF of H-FMT for each distance and for each class corresponds to the right most curve.

VII. Conclusions

We have investigated the use of adaptive MC modulation over WLAN channels and proposed a hybrid architecture based on the use of adaptive OFDM and FMT with minimal length pulses. H-FMT provides significant achievable rate gains over OFDM with a static CP and it has marginal increased complexity.

References

[1] J.A.C. Bingham, "Multicarrier Modulation for data Transmission, an Idea whose Time Has Come," *IEEE Commun. Magazine*, vol. 31, pp. 5-14, May 1990.

[2] G. Cherubini, E. Eleftheriou, S. Olcer, "Filtered Multitone Modulation for Very High-Speed Digital Subscribe Lines," *IEEE J. Sel. Areas Commun.*, pp. 1016-1028, June 2002.

[3] A. M. Tonello, "Performance Limits for Filtered Multitone Modulation in Fading Channels," *IEEE Trans. Wireless Commun.*, vol. 4, no. 5, pp. 2121-2135, Sept. 2005.

[4] A. M. Tonello, "Analytical Results About the Robustness of FMT Modulation with Several Prototype Pulses in Time-Frequency Selective Fading Channels," *IEEE Trans. Wireless Commun.*, vol. 7, no. 5, pp. 1634-1645, May 2008.

[5] W. Kozek, A.F. Molisch, "Nonorthogonal Pulseshapes for Multicarrier Communications in Doubly Dispersive Channels," *IEEE J. Sel. Areas Commun.*, vol. 16, no. 8, pp. 1579-1589, Oct. 1998.

[6] M. Harteneck, S. Weiss, W. Stewart, "Design of Near Perfect Reconstruction Oversampled Filter Banks for Subband Adaptive Filters," *IEEE Trans. on Circuits and Systems Part II: Analog and Digital Signal Processing*, 46 (8). pp. 1081-1086. ISSN 1057-7130, Aug. 1999.

[7] N. Moret, A. M. Tonello, "Design of Orthogonal Filtered Multitone Modulation Systems and Comparison among Efficient Realizations," *EURASIP Journal on Wireless Communications and Networking*, 2010.

[8] J. Seoane, S. Wilson, and S. Gelfand, "Analysis of Intertone and Interblock Interference in OFDM when the Length of the Cyclic Prefix is Shorter than the Length of the Impulse Response of the Channel," *Proc. of IEEE Global Telecomm. Conf. (GLOBECOM)*, Phoenix, USA, Nov. 1997, pp. 32-36.

[9] S. D'Alessandro, A. M. Tonello, L. Lampe, "Improving WLAN Capacity via OFDMA and Cyclic Prefix Adaptation," *Proc. of IEEE IFIP Wireless Days 2009*, Paris, France, Dec. 2009.

[10] V. Ercegl, L. Shumacher et al, IEEE P802.11 Wireless LANs, TGn Channel Models, doc.: IEEE 802.11-03/940r4, May 10, 2004.

[11] A. M. Tonello, "Time Domain and Frequency Domain Implementations of FMT Modulation Architectures," *Proc. of IEEE ICASSP 2006*, Toulose, France, May 2006.

[12] V. Oksman, S. Galli, "G.hn: The New ITU-T Home Networking Standard," *IEEE Commun. Mag.*, vol. 47, no. 10, Oct. 2009, pp. 139–145.

[13] H. Lin, P. Siohan, "Modulation Diversity in Wideband In-Home PLC," in *Proc. of Third Workshop on Powerline Commun. (WSPLC 2009)*, Udine, Italy, Oct. 2009, pp. 86–88.

[14] IEEE Std.802.11, "Wireless LAN Medium Access Control and Physical Layer Specification," Jun. 2007.

[15] A. M. Tonello, S. D'Alessandro, L. Lampe, "Bit, Tone and Cyclic Prefix Allocation in OFDM with Application to In-Home PLC," *Proc. of IEEE IFIP Wireless Days 2008*, Dubai, United Emirates, Nov. 2008, pp. 1–5.